Cell Metabolism, Volume *32*

Supplemental Information

Dynamic Cardiolipin Synthesis

Is Required for CD8$^+$ T Cell Immunity

Mauro Corrado, Joy Edwards-Hicks, Matteo Villa, Lea J. Flachsmann, David E. Sanin, Maaike Jacobs, Francesc Baixauli, Michal Stanczak, Eve Anderson, Mai Azuma, Andrea Quintana, Jonathan D. Curtis, Thomas Clapes, Katarzyna M. Grzes, Agnieszka M. Kabat, Ryan Kyle, Annette E. Patterson, Ramon Klein Geltink, Borko Amulic, Colin G. Steward, Douglas Strathdee, Eirini Trompouki, David O'Sullivan, Edward J. Pearce, and Erika L. Pearce

Figure S1

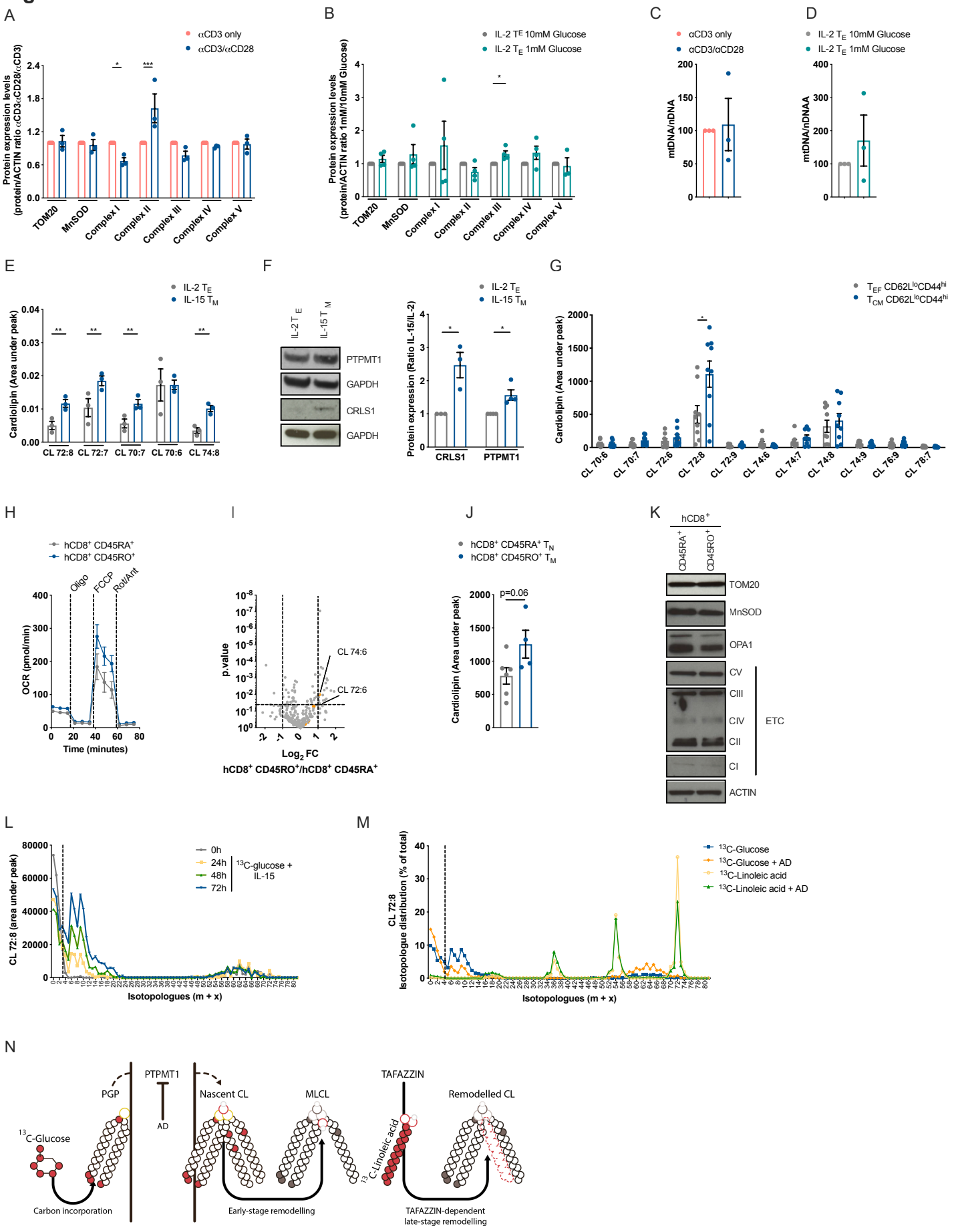
A
αCD3 only
αCD3/αCD28
Protein expression levels (protein/ACTIN ratio αCD3/αCD28/αCD3)
TOM20
MnSOD
Complex I
Complex II
Complex III
Complex IV
Complex V
B
IL-2 TE 10mM Glucose
IL-2 TE 1mM Glucose
Protein expression levels (protein/ACTIN ratio 1mM/10mM Glucose)
C
αCD3 only
αCD3/αCD28
mtDNA/nDNA
D
IL-2 TE 10mM Glucose
IL-2 TE 1mM Glucose
mtDNA/nDNAA
E
IL-2 TE
IL-15 TM
Cardiolipin (Area under peak)
CL 72:8
CL 72:7
CL 70:7
CL 70:6
CL 74:8
F
IL-2 TE
IL-15 TM
PTPMT1
GAPDH
CRLS1
GAPDH
IL-2 TE
IL-15 TM
Protein expression (Ratio IL-15/IL-2)
CRLS1
PTPMT1
G
TEF CD62LloCD44hi
TCM CD62LloCD44hi
Cardiolipin (Area under peak)
CL 70:6
CL 70:7
CL 72:6
CL 72:8
CL 72:9
CL 74:6
CL 74:7
CL 74:8
CL 74:9
CL 76:9
CL 78:7
H
hCD8+ CD45RA+
hCD8+ CD45RO+
Oligo
FCCP
Rot/Ant
OCR (pmol/min)
Time (minutes)
I
p.value
CL 74:6
CL 72:6
Log2 FC
hCD8+ CD45RO+/hCD8+ CD45RA+
J
hCD8+ CD45RA+ TN
hCD8+ CD45RO+ TM
p=0.06
Cardiolipin (Area under peak)
K
hCD8+
CD45RA+
CD45RO+
TOM20
MnSOD
OPA1
CV
CIII
CIV
CII
CI
ETC
ACTIN
L
0h
24h
48h
72h
13C-glucose + IL-15
CL 72:8 (area under peak)
Isotopologues (m + x)
M
13C-Glucose
13C-Glucose + AD
13C-Linoleic acid
13C-Linoleic acid + AD
CL 72:8
Isotopologue distribution (% of total)
Isotopologues (m + x)
N
PTPMT1
PGP
AD
Nascent CL
MLCL
TAFAZZIN
Remodelled CL
13C-Glucose
13C-Linoleic acid
Carbon incorporation
Early-stage remodelling
TAFAZZIN-dependent late-stage remodelling

Figure S1. Mitochondrial protein content and cardiolipin profile in mouse and human CD8$^+$ T cells with a high OXPHOS demand (Related to Figure 1).

(A) Quantification of indicated proteins from immunoblot analysis of CD8$^+$ T cells activated with αCD3 only or αCD3/αCD28 and differentiated into IL-15 T_M cells until day 6 post activation. Quantification refers to representative blot in Figure 2D. Data represent mean ± SEM of four independent experiments.

(B) Quantification of indicated proteins from immunoblot analysis of CD8$^+$ T cells activated with αCD3/αCD28 + IL-2 and cultured in complete medium until day 3, then cultured for 20h in either complete (10mM glucose) or glucose-restricted (1mM glucose) medium for 20h. Quantification refers to representative blot in Figure 2H. Data represent mean ± SEM of four independent experiments.

(C) mtDNA/nDNA ratio measured as ND1/Hprt Ct ratio in cells treated as in (A). Data represent mean ± SEM of three independent experiments.

(D) mtDNA/nDNA ratio measured as ND1/Hprt Ct ratio in cells treated as in (B). Data represent mean ± SEM of three independent experiments.

(E) Cardiolipin species quantification from lipid extracts of CD8$^+$ T cells activated with αCD3/αCD28 and differentiated into IL-2 T_E and IL-15 T_M cells, analyzed by LC-MS. Data represent mean ± SEM of three independent experiments.

(F) Immunoblot analysis and protein quantification of cells activated and differentiated as in Figure 2I. Representative of three independent experiments.

(G) Cardiolipin species quantification from lipids extracts of T_E (CD62L^{lo}CD44^{hi}) and T_M (CD62L^{hi}CD44^{hi}) Wt CD8$^+$ T cells from 20-month old mice. Scatter dot plots with mean ± SEM bars. Dots represent individual mice (n=8-9/group).

(H) OCR of freshly isolated human CD8$^+$ CD45RA$^+$ and CD8$^+$ CD45RO$^+$ T cells at baseline and after exposure to Oligomycin (Oligo), FCCP and Rotenone/Antimycin (Rot/Ant). Data representative of three independent experiments (n=4-5/group)

(I) Lipids extracted from freshly isolated human CD8$^+$ CD45RA$^+$ and CD8$^+$ CD45RO$^+$ T cells and analyzed by LC-MS. Log2FC and p value calculated with Anova test from 4-6 samples per group.

(J) Total cardiolipin content from freshly isolated human CD8$^+$ CD45RA$^+$ and CD8$^+$ CD45RO$^+$ T cells analyzed by LC-MS. Scatter dot plots with mean ± SEM bars. Each dot represents individual donor (n=4-6/group).

(K) Representative immunoblot analysis of cell extracts from freshly isolated human CD8$^+$ CD45RA$^+$ and CD8$^+$ CD45RO$^+$ T cells probed with indicated antibodies.

(L) Isotopologue distribution of ^{13}C-glucose derived carbons incorporated into CL 72:8 in mouse CD8$^+$ T cells differentiated into IL-15 T_M cells in presence of ^{13}C-glucose. At indicated time points lipids were extracted and glucose derived carbons traced into CL 72:8.

(M) Normalized % Isotopologue distribution of ^{13}C-glucose- and ^{13}C-linoleic acid-derived carbons incorporated into CL 72:8 in mouse CD8$^+$ T cells differentiated in IL-15 T_M cells for 72h in presence of ^{13}C-glucose or ^{13}C-palmitate ± cardiolipin synthesis inhibitor (AD) during IL-15 differentiation.

(N) Schematic of glucose- and palmitate/linoleic acid-derived carbons incorporated into cardiolipin.

Statistical comparisons for two groups were calculated by unpaired two-tailed Student's t test or Anova test, where indicated, *p < 0.05; **p < 0.01; ***p < 0.001.

Figure S2

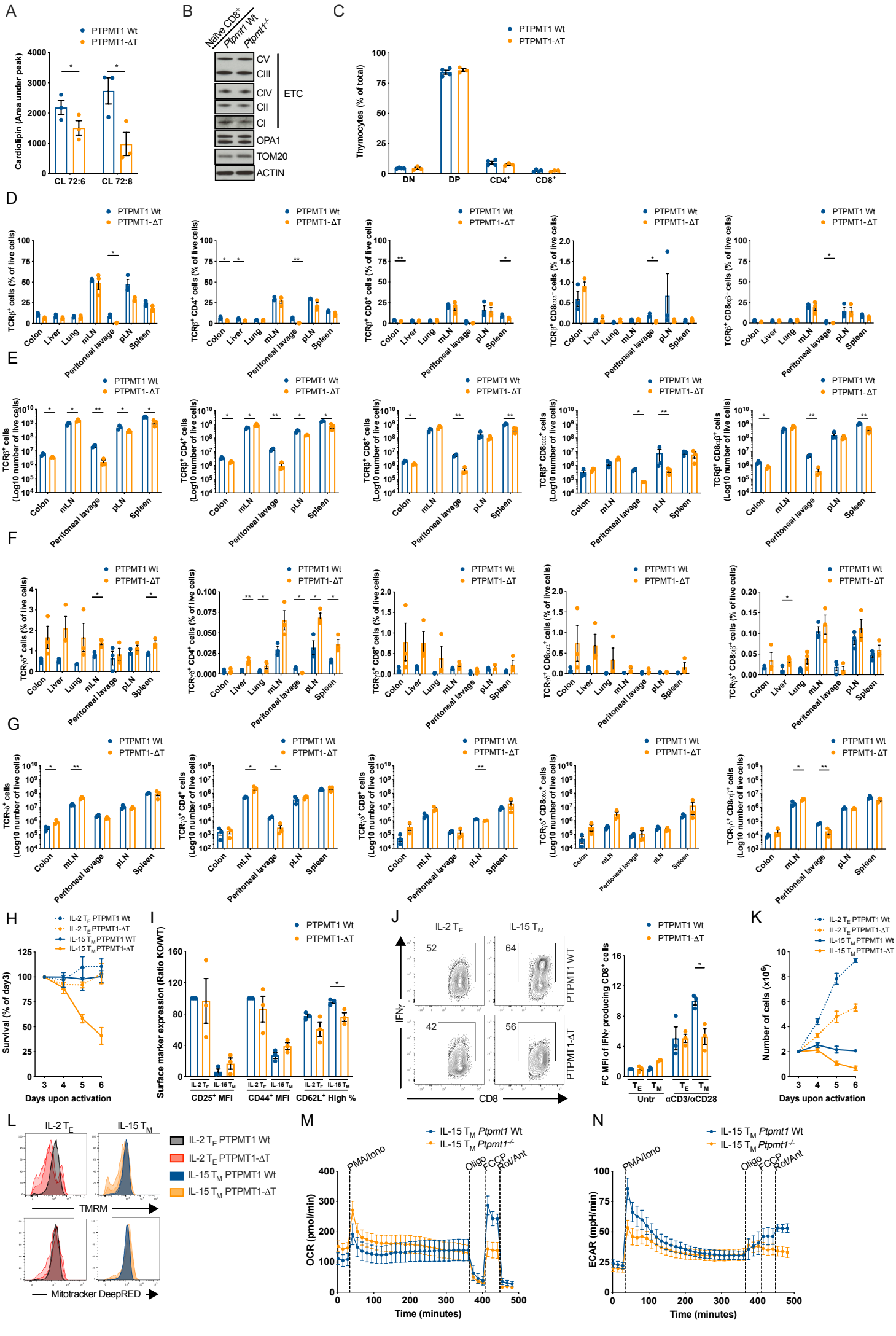
A
PTPMT1 Wt
PTPMT1-ΔT
Cardiolipin (Area under peak)
CL 72:6
CL 72:8
B
Naïve CD8+
Ptpmt1 Wt
Ptpmt1-/-
CV
CIII
CIV
CII
CI
ETC
OPA1
TOM20
ACTIN
C
Thymocytes (% of total)
DN
DP
CD4+
CD8+
D
TCRβ+ cells (% of live cells)
TCRβ+ CD4+ cells (% of live cells)
TCRβ+ CD8+ cells (% of live cells)
TCRβ+ CD8αα+ cells (% of live cells)
TCRβ+ CD8αβ+ cells (% of live cells)
Colon
Liver
Lung
mLN
Peritoneal lavage
pLN
Spleen
E
TCRβ+ cells (Log10 number of live cells)
TCRβ+ CD4+ cells (Log10 number of live cells)
TCRβ+ CD8+ cells (Log10 number of live cells)
TCRβ+ CD8αα+ cells (Log10 number of live cells)
TCRβ+ CD8αβ+ cells (Log10 number of live cells)
F
TCRγδ+ cells (% of live cells)
TCRγδ+ CD4+ cells (% of live cells)
TCRγδ+ CD8+ cells (% of live cells)
TCRγδ+ CD8αα+ cells (% of live cells)
TCRγδ+ CD8αβ+ cells (% of live cells)
G
TCRγδ+ cells (Log10 number of live cells)
TCRγδ+ CD4+ cells (Log10 number of live cells)
TCRγδ+ CD8+ cells (Log10 number of live cells)
TCRγδ+ CD8αα+ cells (Log10 number of live cells)
TCRγδ+ CD8αβ+ cells (Log10 number of live cells)
H
IL-2 TE PTPMT1 Wt
IL-2 TE PTPMT1-ΔT
IL-15 TM PTPMT1 Wt
IL-15 TM PTPMT1-ΔT
Survival (% of day3)
Days upon activation
I
Surface marker expression (Ratio KO/WT)
CD25+ MFI
CD44+ MFI
CD62L+ High %
J
IL-2 TE
IL-15 TM
IFNγ
CD8
52
64
42
56
PTPMT1 WT
PTPMT1-ΔT
FC MFI of IFNγ producing CD8+ cells
Untr
αCD3/αCD28
K
Number of cells (x10^6)
Days upon activation
L
IL-2 TE
IL-15 TM
TMRM
Mitotracker DeepRED
IL-2 TE PTPMT1 Wt
IL-2 TE PTPMT1-ΔT
IL-15 TM PTPMT1 Wt
IL-15 TM PTPMT1-ΔT
M
IL-15 TM Ptpmt1 Wt
IL-15 TM Ptpmt1-/-
PMA/Iono
Oligo
FCCP
Rot/Ant
OCR (pmol/min)
Time (minutes)
N
IL-15 TM Ptpmt1 Wt
IL-15 TM Ptpmt1-/-
PMA/Iono
Oligo
FCCP
Rot/Ant
ECAR (mpH/min)
Time (minutes)

Figure S2. Analysis of WT and Ptpmt1-ΔT mice, and T cells isolated from these mice (Related to Figure 2).

(A) Amount of cardiolipin 72:6 and 72:8 from Wt and *Ptpmt1*-ΔT CD8$^+$ T cells analyzed by LC-MS shown as mean ± SEM. Representative of three experiments (N=3/group).

(B) Immunoblot analysis of cell extracts from naïve WT and *Ptpmt1*-ΔT CD8$^+$ T cells. Representative of two experiments.

(C) Thymocyte development analyzed by CD4/CD8/CD25/CD44 surface expression in 8- week old Wt and PTPMT1-ΔT mice shown as mean ± SEM bars. Dots represent individual mice (n=3-4/group).

(D) % frequencies of TCRβ, TCRβ CD4$^+$, TCRβ CD8$^+$, TCRβ CD8αα$^+$, TCRβ CD8αβ$^+$ T cells in colon, liver, lung, mesenteric lymph nodes (mLN), peritoneal lavage, peripheral lymph node (pLN) and spleens of Wt and PTPMT1-ΔT mice. Data are shown as mean ± SEM bars. Dots represent individual mice (n=3/group).

(E) Cell number expressed in Log10 scale of TCRβ, TCRβ CD4$^+$, TCRβ CD8$^+$, TCRβ CD8αα$^+$, TCRβ CD8αβ$^+$ T cells in colon, mesenteric lymph nodes (mLN), peritoneal lavage, peripheral lymph node (pLN) and spleens of Wt and PTPMT1-ΔT mice. Data are shown as mean ± SEM bars. Dots represent individual mice (n=3/group).

(F) % frequencies of TCRγδ, TCRγδ CD4$^+$, TCRγδ CD8$^+$, TCRγδ CD8αα$^+$, TCRγδ CD8αβ$^+$ T cells in colon, liver, lung, mesenteric lymph nodes (mLN), peritoneal lavage, peripheral lymph node (pLN) and spleens of Wt and PTPMT1-ΔT mice. Data are shown as mean ± SEM bars. Dots represent individual mice (n=3/group).

(G) Cell number expressed in Log10 scale of TCRγδ, TCRγδ CD4$^+$, TCRγδ CD8$^+$, TCRγδ CD8αα$^+$, TCRγδ CD8αβ$^+$ T cells in colon, mesenteric lymph nodes (mLN), perithoneal lavage, peripheral lymph node (pLN) and spleens of Wt and PTPMT1-ΔT mice. Data are shown as mean ± SEM bars. Dots represent individual mice (n=3/group).

(H) Relative survival of WT and *Ptpmt1*$^{-/-}$ CD8$^+$ T cells differentiated in IL-2 (T_E cells) or IL-15 (T_M cells) starting at day 3 post activation. Analyzed by 7-AAD exclusion by flow cytometry. Data represent mean ± SEM of three independent experiment (n=3/group).

(I) CD25, CD44, CD62L expression in Wt and *Ptpmt1*$^{-/-}$ CD8$^+$ T cells cultured for 72h in IL-2 T_E and IL-15 T_M cell conditions. Data represent mean ± SEM of three independent experiments (n=3/group).

(J) Flow cytometry analysis of IFNγ production in IL-2 T_E and IL-15 T_M Wt and *Ptpmt1*$^{-/-}$ CD8$^+$ T cells stimulated for 20h with αCD3/αCD28 antibodies. Graph shows fold change of IFNγ MFI of cytokine producing cells. Data represent mean ± SEM of three independent experiments (n=3/group).

(K) Cell proliferation of mouse Wt and *Ptpmt1*$^{-/-}$ CD8$^+$ T cells measured as cell number between day 3 and day 6 of IL-2 or IL-15 culture, shown as mean ± SEM of 3 independent experiments (n=3/group)

(L) Mitochondrial membrane potential measured with TMRM (upper panel) and mitochondrial mass measured as MitotrackerDeep Red incorporation (lower panel) in IL-2 T_E and IL-15 T_M Wt and *Ptpmt1*$^{-/-}$ CD8$^+$ T cells analyzed by flow cytometry. Representative of 4 Wt and 4 PTPMT1-ΔT mice.

(M) OCR of IL-15 T_M Wt and *Ptpmt1*$^{-/-}$ CD8$^+$ T cells stimulated with PMA/Iono during a Seahorse experiment. Representative of two independent experiment (n=3/group).

(N) Glycolysis measured as extracellular acidification rate (ECAR) in IL-15 T_M Wt and *Ptpmt1*$^{-/-}$ CD8$^+$ T cells stimulated with PMA/Iono during a Seahorse experiment. Representative of two independent experiment (n=3/group).

Statistical comparisons for two groups were calculated by unpaired two-tailed Student's t test, *$p < 0.05$; **$p < 0.01$; ***$p < 0.001$.

Figure S3

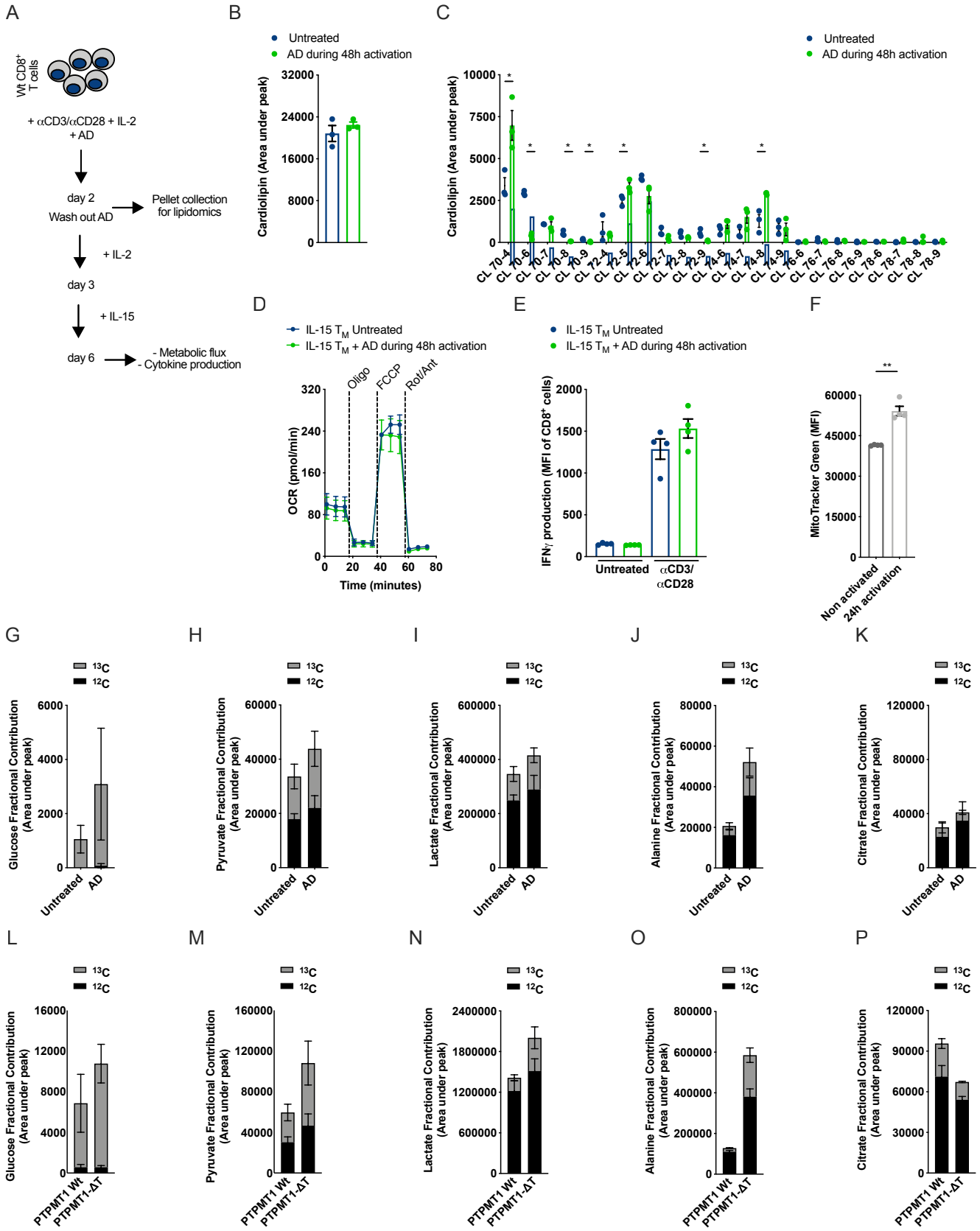
A
Wt CD8+ T cells
+ αCD3/αCD28 + IL-2 + AD
day 2
Wash out AD
Pellet collection for lipidomics
+ IL-2
day 3
+ IL-15
day 6
- Metabolic flux
- Cytokine production
B
Untreated
AD during 48h activation
Cardiolipin (Area under peak)
C
Untreated
AD during 48h activation
Cardiolipin (Area under peak)
D
IL-15 TM Untreated
IL-15 TM + AD during 48h activation
Oligo
FCCP
Rot/Ant
OCR (pmol/min)
Time (minutes)
E
IL-15 TM Untreated
IL-15 TM + AD during 48h activation
IFNγ production (MFI of CD8+ cells)
Untreated
αCD3/ αCD28
F
MitoTracker Green (MFI)
Non activated
24h activation
G
Glucose Fractional Contribution (Area under peak)
H
Pyruvate Fractional Contribution (Area under peak)
I
Lactate Fractional Contribution (Area under peak)
J
Alanine Fractional Contribution (Area under peak)
K
Citrate Fractional Contribution (Area under peak)
L
Glucose Fractional Contribution (Area under peak)
PTPMT1 Wt
PTPMT1-ΔT
M
Pyruvate Fractional Contribution (Area under peak)
N
Lactate Fractional Contribution (Area under peak)
O
Alanine Fractional Contribution (Area under peak)
P
Citrate Fractional Contribution (Area under peak)

Figure S3. ^{13}C-glucose tracing analysis in Wt and *Ptpmt1*$^{-/-}$ CD8^{+} T cells upon activation (Related to Figure 3).

(A) Schematic of CD8^{+} T cells activated with αCD3/αCD28 + IL-2 ± AD for 48h. After 48h AD was washed out and, starting 24h later, cells were differentiated into IL-15 T_M cells.

(B) Total cardiolipin amount CD8^{+} T cells activated and treated as in (A) analyzed by LC-MS. Scatter dot plot represents mean ± SEM (n=3/group).

(C) Cardiolipin species quantification from lipid extracts of CD8^{+} T cells activated and treated as in (A) analyzed by LC-MS. Scatter dot plot represents mean ± SEM (n=3/group).

(D) OCR of CD8^{+} T cells cultured ± AD for 48h during activation activated with αCD3/αCD28 + IL-2 before washing out the inhibitor and differentiating the cells into IL-15 T_M cells. On day 6 post activation the Seahorse experiment was performed. Data represents mean ± SEM of three independent experiments.

(E) IFNγ production measured in IL-15 T_M cells activated and cultured as in (A) and stimulated for 20h with αCD3/αCD28 + IL-2 analyzed by flow cytometry. Data represent mean ± SEM of three independent experiments (n=4/group).

(F) Mitotracker green staining in Wt CD8^{+} cells activated αCD3/αCD28 + IL-2 for 24h. Data are representative of three independent experiments (n=3/group).

(G-K) Fractional contribution of ^{13}C-glucose derived carbons to total amount of indicated metabolites in Wt CD8^{+} T treated with or without AD as described in Figure 3H.

(L-P) Fractional contribution of ^{13}C-glucose derived carbons to total amount of indicated metabolites in Wt and *Ptpmt1*$^{-/-}$ CD8^{+} T cells treated as described in Figure 3J.

Statistical comparisons for two groups were calculated by unpaired two-tailed Student's t test, *$p < 0.05$; **$p < 0.01$; ***$p < 0.001$.

Figure S4

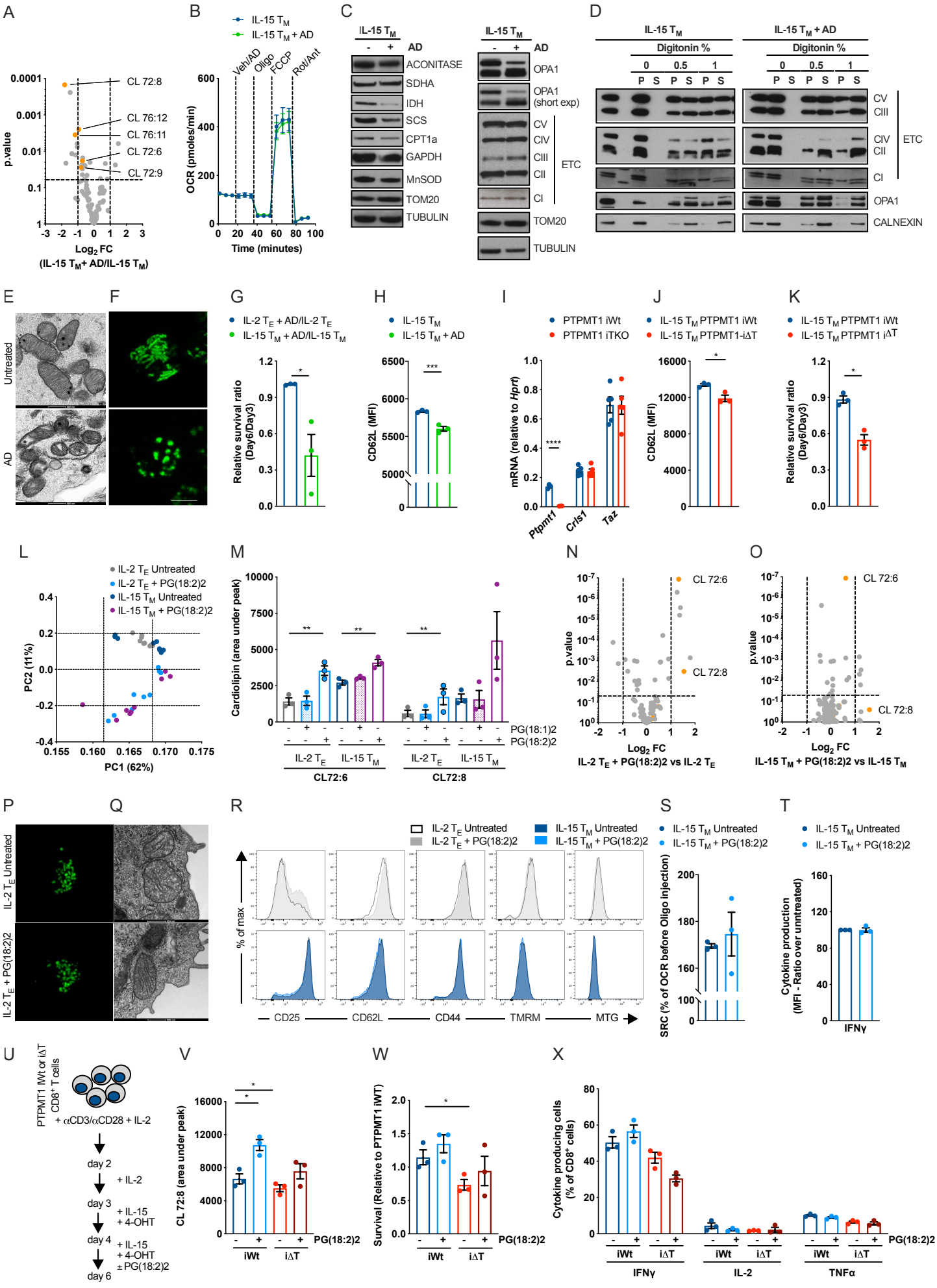
A
p.value
Log2 FC
(IL-15 TM+ AD/IL-15 TM)
CL 72:8
CL 76:12
CL 76:11
CL 72:6
CL 72:9
B
IL-15 TM
IL-15 TM + AD
Veh/AD
Oligo
FCCP
Rot/Ant
OCR (pmoles/min)
Time (minutes)
C
IL-15 TM
AD
ACONITASE
SDHA
IDH
SCS
CPT1a
GAPDH
MnSOD
TOM20
TUBULIN
OPA1
OPA1 (short exp)
CV
CIV
CIII
CII
CI
ETC
D
IL-15 TM
IL-15 TM + AD
Digitonin %
CV
CIII
CIV
CII
CI
ETC
OPA1
CALNEXIN
E
Untreated
AD
F
G
IL-2 TE + AD/IL-2 TE
IL-15 TM + AD/IL-15 TM
Relative survival ratio (Day6/Day3)
H
IL-15 TM
IL-15 TM + AD
CD62L (MFI)
I
PTPMT1 iWt
PTPMT1 iTKO
mRNA (relative to Hprt)
Ptpmt1
Crls1
Taz
J
IL-15 TM PTPMT1 iWt
IL-15 TM PTPMT1-iΔT
CD62L (MFI)
K
IL-15 TM PTPMT1 iWt
IL-15 TM PTPMT1 iΔT
Relative survival ratio (Day6/Day3)
L
IL-2 TE Untreated
IL-2 TE + PG(18:2)2
IL-15 TM Untreated
IL-15 TM + PG(18:2)2
PC2 (11%)
PC1 (62%)
M
Cardiolipin (area under peak)
PG(18:1)2
PG(18:2)2
IL-2 TE
IL-15 TM
CL72:6
CL72:8
N
p.value
CL 72:6
CL 72:8
Log2 FC
IL-2 TE + PG(18:2)2 vs IL-2 TE
O
p.value
CL 72:6
CL 72:8
Log2 FC
IL-15 TM + PG(18:2)2 vs IL-15 TM
P
IL-2 TE Untreated
IL-2 TE + PG(18:2)2
Q
R
IL-2 TE Untreated
IL-2 TE + PG(18:2)2
IL-15 TM Untreated
IL-15 TM + PG(18:2)2
% of max
CD25
CD62L
CD44
TMRM
MTG
S
IL-15 TM Untreated
IL-15 TM + PG(18:2)2
SRC (% of OCR before Oligo injection)
T
IL-15 TM Untreated
IL-15 TM + PG(18:2)2
Cytokine production (MFI - Ratio over unstreated)
IFNγ
U
PTPMT1 iWt or iΔT CD8+ T cells
+ αCD3/αCD28 + IL-2
day 2
+ IL-2
day 3
+ IL-15
+ 4-OHT
day 4
+ IL-15
+ 4-OHT
± PG(18:2)2
day 6
V
CL 72:8 (area under peak)
iWt
iΔT
PG(18:2)2
W
Survival (Relative to PTPMT1 iWt)
iWt
iΔT
PG(18:2)2
X
Cytokine producing cells (% of CD8+ cells)
iWt
iΔT
PG(18:2)2
IFNγ
IL-2
TNFα

Figure S4. Cardiolipin profile, mitochondrial protein levels, morphology, and ultrastructure in CD8$^+$ T cells after AD and PG(18:2) treatment (Related to Figure 4).

(A) Lipids extracted from IL-15 T_M CD8$^+$ T cells cultured as in Figure 3A and analyzed by LC-MS. Log2FC and p value calculated with Anova test from 3 samples per group.

(B) OCR of IL-15 T_M CD8$^+$ T cells at baseline and after exposure to Vehicle/AD, Oligomycin (Oligo), FCCP, and Rotenone/Antimycin (Rot/Ant). Data representative of three independent experiments (n=3/group).

(C) Immunoblot analysis of Wt IL-15 T_M CD8$^+$ T cells cultured ± AD for 72h.

(D) Immunoblot analysis of CALNEXIN, OPA1 and ETC complexes (CI-NDUFB8, CII-SDHB, CIII-UQCRC2, CIV-MTC01, CV-ATP5A). Equivalent numbers of IL-15 T_M cells cultured ± AD for 72h were lysed in native lysis buffer followed by digitonin solubilization of intracellular membranes with pellet (P) and solubilized supernatant (S) fractions resolved on a denaturing gel, representative of two experiments.

(E) Representative electron micrographs of mouse IL-15 T_M CD8$^+$ T cells cultured ± AD for 72h. Scale bars: 500nm.

(F) Representative mitochondrial morphology of live IL-15 T_M CD8$^+$ T cells isolated form PhAM mice cultured ± AD for 72h analyzed by spinning disk confocal microscopy. Scale bar: 5μm

(G) Relative survival ratio of IL-2 T_E and IL-15 T_M cells cultured± AD for 72h starting at day 3 post activation analyzed by 7-AAD exclusion by flow cytometry. Data represent mean ± SEM of three independent experiments (n=3/group).

(H) CD62L expression in mouse IL-15 T_M cells cultured in ± AD for 72h analyzed by flow cytometry. Data represent mean ± SEM of three independent experiments (n=3/group).

(I) CD8$^+$ T cells were isolated from *Ptpmt1*$^{flox/flox}$Ert2-Cre$^{-/-}$ (PTPMT1 iWt) *Ptpmt1*$^{flox/flox}$Ert2-Cre$^{+/-}$ (PTPMT1 iΔT) mice. Efficiency of *Ptpmt1*deletion by Cre recombinase, *Crls1* and *Taz* expression levels measured after iWt and iΔT cells were cultured in IL-15 in presence of 4-OHT for 72h analyzed by qPCR shown as mean ± SEM (n=3/group).

(J) CD62L expression in mouse *Ptpmt1* iWt and *Ptpmt1* iΔT CD8$^+$ T cells cultured as in Figure 3E analyzed by flow cytometry. Data represent mean ± SEM of three independent experiments (n=3/group).

(K) Relative survival of IL-15 T_M PTPMT1 iΔT versus IL-15 T_M PTPMT1 iWt T cells cultured with 4-OHT for 72h starting at day 3 post activation and analyzed by 7-AAD exclusion by flow cytometry. Data represent mean ± SEM of three independent experiments (n=3/group).

(L) PCA analysis of lipids extracted from CD8$^+$ T cells differentiated into IL-2 T_E and IL-15 T_M cells ± PG(18:2)2 and analyzed by LC-MS.

(M) Cardiolipin species quantification from lipids extracts from IL-15 T_M CD8$^+$ T cells cultured as in (N) analyzed by LC-MS. Data represent mean ± SEM of three independent experiments.

(N-O) Lipids extracted from CD8$^+$ T cells differentiated into IL-2 T_E or IL-15 T_M cells ± PG(18:2)2 and analyzed by LC-MS. Log2FC and p value calculated with Anova test from 9 samples per group.

(P-Q) Representative mitochondrial morphology of live CD8$^+$ T cells analyzed by spinning disk confocal and representative electron micrographs of mouse IL-2 T_E CD8$^+$ T cells cultured in IL-2 in the presence of BSA-conjugated 50μM PG(18:2)2 for 48h. Scale bars: 5μm confocal, 500nm EM.

(R) Representative histogram plots depicting surface expression of CD25, CD62L, CD44 together with TMRM and Mitotracker green staining in mouse IL-2 T_E and IL-15 T_M CD8$^+$ T cells untreated or cultured in the presence of BSA-conjugated 50μM PG(18:2)2 for 48h.

(S) SRC of mouse IL-15 T_M CD8$^+$ T cells cultured ± PG(18:2)2 for 48h stimulated with αCD3/αCD28 coated beads in a Seahorse Extracellular Flux Analyzer. Data represent mean ± SEM of three independent experiments (n=3/group).

(T) Cytokine production (normalized to untreated cells) measured in IL-15 T_M CD8$^+$ T cells activated as in (I) and stimulated for 20h with αCD3/αCD28 + IL-2. Data represent mean ± SEM of two or three independent experiment (n=3/group).

(U) Schematic of mouse *Ptpmt1* iWt and *Ptpmt1* iΔT CD8$^+$ T cells activated with αCD3/αCD28 + IL-2 for 24, cultured in IL-2 for additional 24h. 4-OHT was supplemented starting form day3 post activation together with IL-15. From day4 to day 6 post activation cells were cultured in the presence of BSA-conjugated 50μM PG(18:2)2 for 48h.

(V) Quantification of CL 72:8 content in IL-15 T_M cells cultured as in (U) and analyzed by LC-MS. Scatter dot plots with mean ± SEM of three independent experiments (n=3/group).

(W) Relative survival of IL-15 T_M PTPMT1 iΔT versus IL-15 T_M PTPMT1 iWt T cells cultured as in (U) and analyzed by 7-AAD exclusion by flow cytometry. Data represent mean ± SEM of three independent experiments (n=3/group).

(X) Cytokine production measured in IL-15 T_M CD8$^+$ T cells cultured as in (U) and stimulated for 20h with αCD3/αCD28 + IL-2. Data represent mean ± SEM of three independent experiment (n=3/group).

Statistical comparisons for two groups were calculated by unpaired two-tailed Student's t test or Anova test, where indicated, *p < 0.05; **p < 0.01; ***p < 0.001.

Figure S5

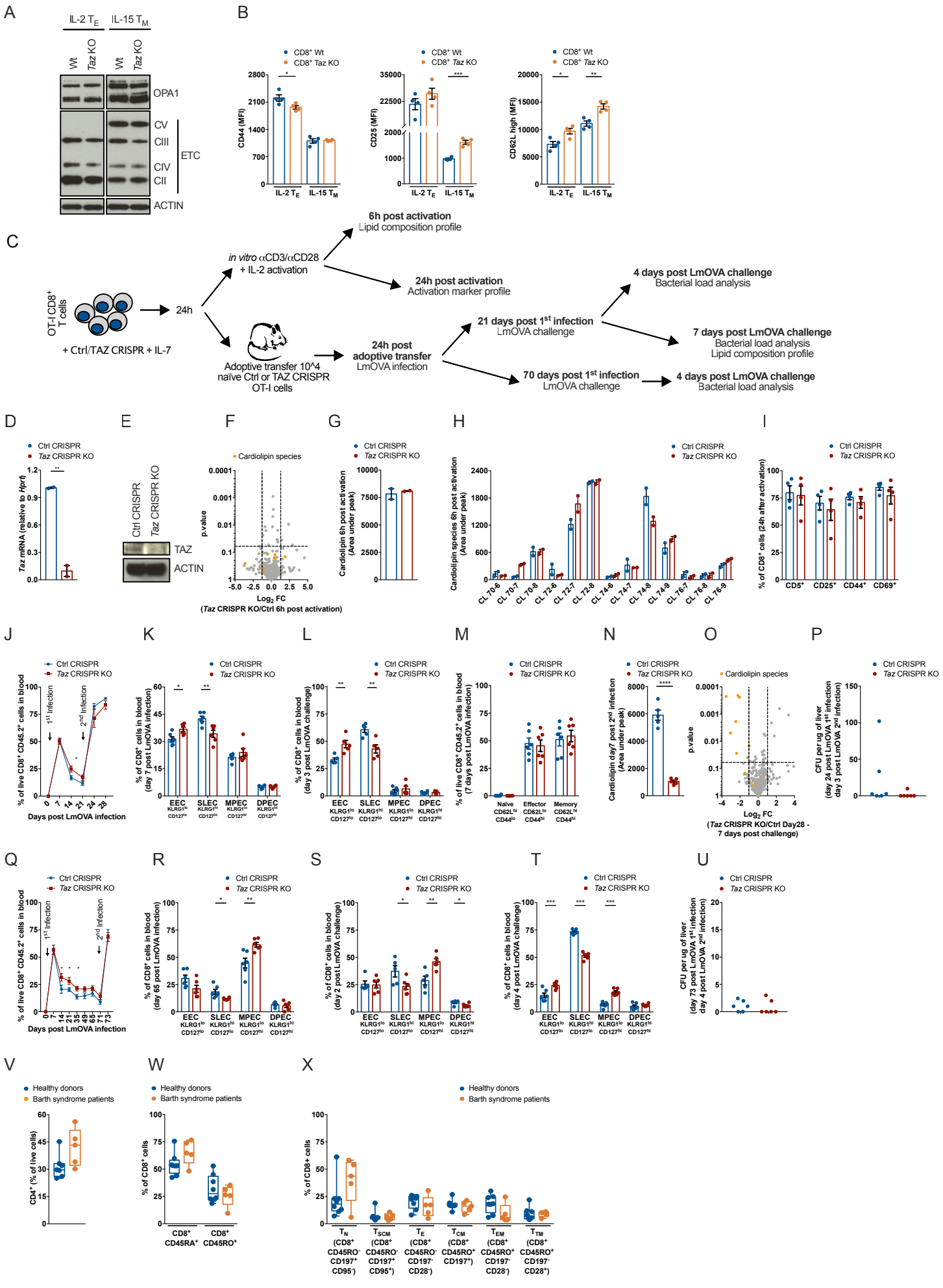
A
IL-2 T_E
IL-15 T_M
Wt
Taz KO
OPA1
CV
CIII
CIV
CII
ETC
ACTIN
B
CD8+ Wt
CD8+ Taz KO
CD44 (MFI)
CD25 (MFI)
CD62L high (MFI)
C
OT-I CD8+ T cells
+ Ctrl/TAZ CRISPR + IL-7
24h
in vitro αCD3/αCD28 + IL-2 activation
6h post activation
Lipid composition profile
24h post activation
Activation marker profile
Adoptive transfer 10^4 naïve Ctrl or TAZ CRISPR OT-I cells
24h post adoptive transfer
LmOVA infection
21 days post 1st infection
LmOVA challenge
4 days post LmOVA challenge
Bacterial load analysis
7 days post LmOVA challenge
Bacterial load analysis
Lipid composition profile
70 days post 1st infection
LmOVA challenge
4 days post LmOVA challenge
Bacterial load analysis
D
Ctrl CRISPR
Taz CRISPR KO
Taz mRNA (relative to Hprt)
E
Ctrl CRISPR
Taz CRISPR KO
TAZ
ACTIN
F
Cardiolipin species
p.value
Log2 FC
(Taz CRISPR KO/Ctrl 6h post activation)
G
Cardiolipin 6h post activation (Area under peak)
H
Cardiolipin species 6h post activation (Area under peak)
I
% of CD8+ cells (24h after activation)
CD5+
CD25+
CD44+
CD69+
J
% of live CD8+ CD45.2+ cells in blood
1st Infection
2nd Infection
Days post LmOVA infection
K
% of CD8+ cells in blood (day 7 post LmOVA infection)
EEC KLRG1lo CD127lo
SLEC KLRG1hi CD127lo
MPEC KLRG1lo CD127hi
DPEC KLRG1hi CD127hi
L
% of CD8+ cells in blood (day 3 post LmOVA challenge)
M
% of live CD8+ CD45.2+ cells in blood (7 days post LmOVA infection)
Naïve CD62Lhi CD44lo
Effector CD62Llo CD44hi
Memory CD62Lhi CD44hi
N
Cardiolipin day7 post 2nd infection (Area under peak)
O
Cardiolipin species
p.value
Log2 FC
(Taz CRISPR KO/Ctrl Day28 - 7 days post challenge)
P
CFU per ug of liver (day 24 post LmOVA 1st infection day 3 post LmOVA 2nd infection)
Q
% of live CD8+ CD45.2+ cells in blood
1st Infection
2nd Infection
Days post LmOVA infection
R
% of CD8+ cells in blood (day 65 post LmOVA infection)
S
% of CD8+ cells in blood (day 2 post LmOVA challenge)
T
% of CD8+ cells in blood (day 4 post LmOVA challenge)
U
CFU per ug of liver (day 73 post LmOVA 1st infection day 4 post LmOVA 2nd infection)
V
Healthy donors
Barth syndrome patients
CD4+ (% of live cells)
W
% of CD8+ cells
CD8+ CD45RA+
CD8+ CD45RO+
X
% of CD8+ cells
TN (CD8+ CD45RO- CD197+ CD95-)
TSCM (CD8+ CD45RO- CD197+ CD95+)
TE (CD8+ CD45RO- CD197- CD28-)
TCM (CD8+ CD45RO+ CD197+)
TEM (CD8+ CD45RO+ CD197- CD28-)
TTM (CD8+ CD45RO+ CD197- CD28+)

Figure S5. T cell defects in TAK KO mice are not T cell intrinsic (Related to Figure 5).

(A) Immunoblot analysis of cell extracts of $CD8^+$ T cells from 20-week old Wt and *Tafazzin* KO mice activated with αCD3/αCD28 + IL-2 and differentiated into IL-2 T_E or IL-15 T_M cells for 72h starting day 3 post activation.

(B) CD44, CD25, CD62L expression in $CD8^+$ T cells from 20 week old Wt and *Tafazzin* KO mice activated with αCD3/αCD28 + IL-2 and differentiated in IL-2 T_E or IL-15 T_M cells for 72h starting day 3 post activation analyzed by flow cytometry. Data representative of 3 independent experiments shown as mean ± SEM (n=4/group).

(C) Schematic of experimental setup. Naïve OT-I cells were ctrl (Ctrl CRISPR) or *Tafazzin* (*Taz* CRISPR KO) CRISPRed, followed by 24 a rest period in IL-7. After 24h cells were either *in vitro* activated and lipids and activation markers analyzed at indicated time points, or adoptively transferred *in vivo* into congenic mice, which were then infected 24h later i.v. with $1x10^6$ CFU LmOVA ΔActa and followed as indicated. After 21 days (or 70 days), mice were challenged i.v. with LmOVA Wt or ΔActa, Donor cells frequencies and bacterial analyzed post challenge as indicated.

(D) *Tafazzin* expression in OT-I cells 24h after CRISPR, analyzed by qPCR shown as mean ± SEM (n=2/group).

(E) *Tafazzin* expression in OT-I cells 24h after CRISPR, analyzed by Wb.

(F) Lipids extracted from Ctrl CRISPR and *Taz* CRISPR KO OT-I cells 6h after activation with αCD3/αCD28 + IL-2, analyzed by LC-MS. Data show Log2FC and p value calculated with Anova test from two samples per condition per time point.

(G) Total cardiolipin amount in Ctrl CRISPR and *Taz* CRISPR KO OT-I cells 6h after activation with αCD3/αCD28 + IL-2 analyzed by LC-MS. Data show mean ± SEM and p value calculated with Anova test from two samples per condition per time point.

(H) Cardiolipin species quantification from lipid extracts of Ctrl CRISPR and *Taz* CRISPR KO OT-I cells 6h after activation with αCD3/αCD28 + IL-2 analyzed by LC-MS. Scatter dot plots with mean ± SEM bars (n=2/group).

(I) CD5, CD44, CD25, CD69 expression in Ctrl CRISPR and *Taz* CRISPR KO OT-I cells 24h after activation with αCD3/αCD28 + IL-2, analyzed by flow cytometry. Data from 4 independent CRISPR experiments shown as mean ± SEM.

(J) % of Ctrl CRISPR and *Taz* CRISPR KO OT-I $CD8^+$ $CD45.2^+$ donor cells in congenic mice infected i.v. with 10^6 CFU LmOVA ΔActa shown as mean ± SEM. Representative of two experiments (n=6/group).

(K) EEC, SLEC, MPEC and DPEC Ctrl CRISPR and *Taz* CRISPR KO OT-I $CD8^+$ $CD45.2^+$ donor cells 7 days after primary infection analyzed according to KLRG1 and CD127 surface expression shown as mean ± SEM bars. Representative of two independent experiments (n=6/group).

(L) EEC, SLEC, MPEC and DPEC Ctrl CRISPR and *Taz* CRISPR KO OT-I $CD8^+$ $CD45.2^+$ donor cells 3 days after secondary infection analyzed according to KLRG1 and CD127 surface expression shown as mean ± SEM bars. Representative of two independent experiments (n=6/group).

(M) % of naïve ($CD62L^{hi}CD44^{lo}$), T_E ($CD62L^{lo}CD44^{hi}$) and T_M ($CD62L^{hi}CD44^{hi}$) $CD8^+$ $CD45.2^+$ donor Ctrl CRISPR and *Taz* CRISPR KO OT-I cells 7 days after primary infection analyzed by flow cytometry shown as mean ± SEM bars. Scatter dot plot represents mean ± SEM. Dots represent individual mice (n=6/group).

(N) Total cardiolipin amount in Ctrl CRISPR and *Taz* CRISPR KO OT-I cells 7 days after secondary infection analyzed by LC-MS. Scatter dot plots with mean ± SEM bars (n=5/group).

(O) Lipids extracted from Ctrl CRISPR and *Taz* CRISPR KO OT-I cells sorted from recipient mice 7 days after LmOVA ΔActa challenge. Data show Log2FC and p value calculated with Anova test from 6 samples per group.

(P) Bacterial burden shown as CFU per µg of liver isolated from mice adoptively transferred with Ctrl CRISPR and *Taz* CRISPR KO OT-I cells 3 days post LmOVA challenge. Each dot represents individual mice (n=6/group).

(Q) % of Ctrl CRISPR and *Taz* CRISPR KO OT-I $CD8^+$ $CD45.2^+$ donor cells in congenic mice infected i.v. with 10^6 CFU LmOVA ΔActa shown as mean ± SEM (n=6/group).

(R-T) EEC, SLEC, MPEC and DPEC Ctrl CRISPR and *Taz* CRISPR KO OT-I $CD8^+$ $CD45.2^+$ donor cells 65 days after primary infection (R), 2 days (S) and 4 days (T) after secondary infection analyzed according to KLRG1 and CD127 surface expression shown as mean ± SEM bars. Dots represent individual mice (n=6/group).

(U) Bacterial burden shown as CFU per µg of liver isolated from mice adoptively transferred with Ctrl CRISPR and *Taz* CRISPR KO OT-I cells 4 days post LmOVA challenge. Each dot represents individual mice (n=6/group).

(V) % of $CD4^+$ T cells in hPBMCs from healthy donors and Barth Syndrome patients. Dots are individual donors.

(W) $CD45RA^+$ and $CD45RO^+$ expression in $CD8^+$ T cells from healthy donors and Barth Syndrome patients. Dots are individual donors.

(X) $CD8^+$ T naïve (T_N), T stem cell memory (T_{SCM}), T effector (T_E), T central memory (T_{CM}), T effector memory (T_{EM}), T transition memory (T_{TM}) analyzed according to CD8, CD45RO, CD197, CD95, CD28 expression as indicated was analyzed by flow cytometry. Dots are individual donors.

Statistical comparisons for two groups were calculated by unpaired two-tailed Student's t test or Anova test, where indicated, *p < 0.05; **p < 0.01; ***p < 0.001.